

Effects of ϕ and σ^* -meson on properties of hyperon stars including Δ resonance

Fu Ma^{1,2}, Chen Wu³ and Wenjun Guo⁴

1. Key Laboratory of Nuclear Physics and Ion-beam Application (MOE), Institute of Modern Physics, Fudan University, Shanghai 200433, China
2. Shanghai Research Center for Theoretical Nuclear Physics (NSFC), Fudan University, Shanghai 200438, China
3. Shanghai Advanced Research Institute, Chinese Academy of Sciences, Shanghai 201210, China
4. University of Shanghai for Science and Technology, Shanghai 200093, China

In this work, we study the properties of neutron stars using the linear Relativistic Mean-Field (RMF) theory and consider multiple degrees of freedom inside neutron stars, including hyperons and Δ resonances. We investigate different coupling parameters $x_{\sigma\Delta}$ between Δ resonances and nucleons and compare the differences between neutron stars with and without strange mesons σ^* and ϕ . These effects include particle number distributions, equations of state (EOS), mass-radius relations, and tidal deformabilities. To overcome the "hyperon puzzle," we employ the σ -cut scheme to obtain neutron stars with masses up to $2M_\odot$. We find that strange mesons appear at around $3\rho_0$ and reduce the critical density of baryons in the high-density region. With increasing coupling parameter $x_{\sigma\Delta}$, the Δ resonances suppress hyperons, leading to a shift of the critical density towards lower values. The early appearance of Δ resonances may play a crucial role in the stability of neutron stars. Strange mesons soften the EOS slightly, while Δ resonances predominantly soften the EOS in the low-density region. By calculating tidal deformabilities and comparing with astronomical observation GW170817, we find that the inclusion of Δ resonances decreases the radius of neutron stars.

I. INTRODUCTION

Observations of massive neutron stars, such as PSR J1614-2230 with a mass of $1.908 \pm 0.016M_\odot$, have provided important constraints on the equation of state (EOS) of nuclear matter [1–4]. Similarly, PSR J0348+0432 with a mass of $2.01 \pm 0.04M_\odot$ [5], MSP J0740+6620 with a mass of $2.08_{-0.07}^{+0.07}M_\odot$ [6, 7] and a radius of $12.39_{-0.98}^{+1.30}$ km (from NICER observations [8]) have also contributed to constraining the EOS. The first multi-messenger gravitational wave event GW170817 observed by LIGO-Virgo Collaboration (LVC) set constraints on the tidal deformability [9, 10] of the involved stars. The compactness-radius relation predicts a radius of $12 \leq R_{1.4} \leq 13$ km for a standard mass neutron star with $M = 1.4M_\odot$. These astronomical observations not only constrain the tidal deformability of a $1.4 M_\odot$ neutron star but also shed light on the strong interactions within dense nuclear matter.

Due to the high core density inside neutron stars, as the nucleon density increases, the strong interaction among hadrons leads to the excitation of hyperons [11–14], Δ resonances [15–23], or kaon meson condensation [24–28] in the neutron star interior. These forms of matter have significant impacts on the structure and evolution of the stars. While the presence of hyperons inside neutron stars is unavoidable, their appearance results in a significant softening of the equation of state, leading to a reduction in the maximum mass of neutron stars, commonly referred to as the hyperon puzzle [29–31]. Despite various speculations about the existence of hyperons in neutron stars, discussions about Δ resonances have been limited. This is because the coupling parameters of Δ with nucleons are not well determined, either experimentally or theoretically, and different coupling parameters

can have a significant impact on the final results [20, 32]. Additionally, the occurrence of Δ resonances causes the equation of state to soften, giving rise to a Δ puzzle, similar to the hyperon puzzle found in some literature [19]. To ensure the stiffness of the equation of state and the existence of massive neutron stars, researchers have employed linear RMF theory with the inclusion of the sigma-cut scheme [33] and density-dependent functionals to study neutron stars containing hyperons [19, 34–39].

The resolution of the hyperon puzzle requires additional repulsive interactions between baryons [40] to counteract this attractive mechanism. These repulsive interactions include: (a) Increasing the repulsive hyperon three-body force [30]. (b) Deconfinement phase transition to quark matter below the hyperon threshold [41]. (c) Enhancing the repulsive hyperonic interactions through the exchange of vector mesons [42]. The Relativistic Mean-Field (RMF) theory is an effective field theory used to handle the interactions between hadrons (nucleons) in a relativistic framework. The relevant degrees of freedom in this theory are baryons interacting through the exchange of σ , ω , and ρ mesons. The scalar meson σ provides intermediate-range attraction, the vector meson ω provides short-range repulsion, and the vector-isovector meson ρ describes the difference between neutrons and protons. Over the years, the σ , ω , and ρ mesons have been widely applied in various aspects of neutron star research. However, there should also be scalar meson σ^* and vector meson ϕ involved in the interactions between hyperons. These two mesons specifically interact between hyperons and do not participate in interactions between nucleons. In this work, we employ an alternative approach to overcome the softening of the equation of state (EOS) caused by multiple degrees of freedom, namely the σ -cut scheme [33]. This scheme suggests that

TABLE I. Strangeness mass M , third component of isospin τ_3 , charge q , total angular momentum and parity J^P for Λ^0 , $\Sigma^{+,0,-}$ and $\Xi^{-,0}$ hyperons and Δ baryons.

	$M(MeV)$	τ_3	$q(e)$	J^P
Λ^0	1116	0	0	$(1/2)^+$
Σ^+	1193	1	+1	$(1/2)^+$
Σ^0	1193	0	0	$(1/2)^+$
Σ^-	1193	-1	-1	$(1/2)^+$
Ξ^0	1318	$(1/2)$	0	$(1/2)^+$
Ξ^-	1318	$(-1/2)$	-1	$(1/2)^+$
Δ^{++}	1232	$(+3/2)$	+2	$(3/2)^+$
Δ^+	1232	$(+1/2)$	+1	$(3/2)^+$
Δ^0	1232	$(-1/2)$	0	$(3/2)^+$
Δ^-	1232	$(-3/2)$	-1	$(3/2)^+$

in the small-scale range where the density $\rho_B > \rho_0$, a sharp decrease in the strength of the σ meson reduces the drop

in the effective mass of nucleons, leading to an increase in the particle chemical potential and ultimately resulting in the stiffening of the EOS [43, 44]. In this article, we use the IUFSU model [45, 46] to study neutron star matter including hyperons, Δ resonance, and strange mesons (σ^* , ϕ) with the σ -cut scheme. In Table I, we present the properties and fundamental constants for baryons other than nucleons.

This paper is organized as follows. First, the theoretical framework is presented. Then we will study the effects of strange mesons (σ^* , ϕ) and Δ resonance contains hyperons with the σ -cut scheme. Finally, some conclusions are provided.

II. THEORETICAL FRAMEWORK

In this section, we introduce the IUFSU model to study the properties of the NS including hyperons and Δ resonance, the Lagrangian density of hadron matter is given by:

$$\begin{aligned}
\mathcal{L} = & \sum_B \bar{\psi}_B [i\gamma^\mu \partial_\mu - m_B + g_{\sigma B} \sigma - g_{\omega B} \gamma^\mu \omega_\mu - g_{\phi B} \gamma^\mu \phi_\mu - g_{\rho B} \gamma^\mu \vec{\tau} \cdot \vec{\rho}^\mu] \psi_B + \\
& \sum_D \bar{\psi}_D [i\gamma^\mu \partial_\mu - m_D + g_{\sigma D} \sigma - g_{\omega D} \gamma^\mu \omega_\mu - g_{\phi D} \gamma^\mu \phi_\mu - g_{\rho D} \gamma^\mu \vec{\tau} \cdot \vec{\rho}^\mu] \psi_D + \\
& \frac{1}{2} \partial_\mu \sigma \partial^\mu \sigma - \frac{1}{2} m_\sigma^2 \sigma^2 - \frac{\kappa}{3!} (g_{\sigma N} \sigma)^3 - \frac{\lambda}{4!} (g_{\sigma N} \sigma)^4 - \frac{1}{4} F_{\mu\nu} F^{\mu\nu} + \frac{1}{2} m_\omega^2 \omega_\mu \omega^\mu - \\
& \frac{1}{4} \Phi_{\mu\nu} \Phi^{\mu\nu} + \frac{1}{2} m_\phi^2 \phi_\mu \phi^\mu + \frac{\xi}{4!} (g_{\omega N}^2 \omega_\mu \omega^\mu)^2 + \frac{1}{2} m_\rho^2 \vec{\rho}^\mu \cdot \vec{\rho}^\mu - \frac{1}{4} \vec{G}_{\mu\nu} \vec{G}^{\mu\nu} + \\
& \frac{1}{2} (\partial_\mu \sigma^* \partial^\mu \sigma^* - m_{\sigma^*}^2 \sigma^{*2}) + \Lambda_\nu (g_{\rho N}^2 \vec{\rho}^\mu \cdot \vec{\rho}^\mu) (g_{\omega N}^2 \omega_\mu \omega^\mu) + \sum_l \bar{\psi}_l [i\gamma^\mu \partial_\mu - m_l] \psi_l,
\end{aligned} \tag{1}$$

with the field tensors

$$\begin{aligned}
F_{\mu\nu} &= \partial_\mu \omega_\nu - \partial_\nu \omega_\mu \\
\Phi_{\mu\nu} &= \partial_\mu \phi_\nu - \partial_\nu \phi_\mu \\
\vec{G}_{\mu\nu} &= \partial_\mu \rho_\nu - \partial_\nu \rho_\mu,
\end{aligned} \tag{2}$$

The model includes the baryon octet and two leptons ($p, n, e, \mu, \Lambda^0, \Sigma^+, \Sigma^0, \Sigma^-, \Xi^0, \Xi^-$) as well as Δ resonances ($\Delta^{++}, \Delta^+, \Delta^0, \Delta^-$). The strong interactions between baryons are mediated by the isoscalar-scalar mesons σ , σ^* , isoscalar-vector mesons ω , ϕ and isovector-vector me-

son ρ , each with their respective masses and coupling constants. The isospin operator $\vec{\tau}$ is used to represent the isovector-vector meson fields. The parameter Λ_ν is introduced to modify the density dependence of the symmetry energy. The self-interactions of the isoscalar mesons (through the κ , λ , and ξ terms) are necessary to obtain an appropriate equation of state for symmetric nuclear matter. In the relativistic mean field (RMF) model, the operators of the meson fields are replaced by their expectation values using the mean field approximation. The parameters of the IUFSU model are listed in Table II.

Finally, with the Euler-Lagrange equation, the equations of motion for baryons and mesons are obtained:

$$\begin{aligned}
m_\sigma^2 \sigma + \frac{1}{2} \kappa g_{\sigma N}^3 \sigma^2 + \frac{1}{6} \lambda g_{\sigma N}^4 \sigma^3 &= \sum_B g_{\sigma B} \rho_B^S + \sum_D g_{\sigma D} \rho_D^S \\
m_\omega^2 \omega + \frac{\xi}{6} g_{\omega N}^4 \omega^3 + 2\Lambda_\nu g_{\rho N}^2 g_{\omega N}^2 \rho^2 \omega &= \sum_B g_{\omega B} \rho_B + \sum_D g_{\omega D} \rho_D \\
m_\rho^2 \rho + 2\Lambda_\nu g_{\rho N}^2 g_{\omega N}^2 \omega^2 \rho &= \sum_B g_{\rho B} \tau_{3B} \rho_B + \sum_D g_{\rho D} \tau_{3D} \rho_D \\
m_\phi^2 \phi &= \sum_B g_{\phi B} \rho_B \\
m_{\sigma^*}^2 \sigma^* &= \sum_B g_{\sigma^* B} \rho_B^S,
\end{aligned} \tag{3}$$

where $\rho_{B(D)}$ and $\rho_{B(D)}^S$ are the baryon(Δ) density and the scalar density, which reads:

$$\begin{aligned}
\rho_B &= \frac{\gamma k_{fB}}{6\pi^2} \\
\rho_B^S &= \frac{\gamma M^*}{4\pi^2} [k_{fB} E_{fB}^* - M^{*2} \ln(\frac{k_{fB} + E_{fB}^*}{M^{*2}})]
\end{aligned} \tag{4}$$

$\gamma = 2$ for baryons and $\gamma = 4$ for Δ resonance. where $E_{fB}^* = \sqrt{k_{fB}^2 + M^{*2}}$.

Now, we are in a position to discuss the coupling parameters between baryons (nucleons, hyperons and Δ) and meson fields.

For the meson-hyperon couplings, we take those in the SU(6) symmetry for the vector couplings constants:

$$\begin{aligned}
g_{\rho\Lambda} &= 0, g_{\rho\Sigma} = 2g_{\rho\Xi} = 2g_{\rho N} \\
g_{\omega\Lambda} &= g_{\omega\Sigma} = 2g_{\omega\Xi} = \frac{2}{3}g_{\omega N} \\
2g_{\phi\Lambda} &= 2g_{\phi\Sigma} = g_{\phi\Xi} = \frac{-2\sqrt{2}}{3}g_{\omega N}
\end{aligned} \tag{5}$$

The scalar couplings are typically determined by fitting hyperon potentials with $U_Y^{(N)} = g_{\omega Y} \omega_0 - g_{\sigma Y} \sigma_0$, where σ_0 and ω_0 are the values of the scalar and vector meson strengths at nuclear saturation density [47]. We choose the hyperon-nucleon potentials of Λ , Σ , and Ξ as $U_\Lambda^N = -30\text{MeV}$, $U_\Sigma^N = 30\text{MeV}$, and $U_\Xi^N = -18\text{MeV}$ [48-50]. Table III provides the numerical values of the meson-hyperon couplings at nuclear saturation density, where $x_{\sigma Y} = g_{\sigma Y}/g_{\sigma N}$.

While strange mesons only interact with hyperons, so $g_{\phi N} = g_{\sigma^* N} = g_{\phi\Delta} = g_{\sigma^*\Delta} = 0$. The masses of the strange mesons ϕ and σ^* are $M_\phi = 1020\text{MeV}$ and $M_{\sigma^*} = 975\text{MeV}$, respectively.

For the scalar meson σ^* , we treat its coupling purely phenomenologically so as to satisfy the potential depths $U_\Sigma^{(\Xi)} \simeq U_\Lambda^{(\Xi)} \simeq U_\Xi^{(\Xi)} \simeq U_\Lambda^{(\Lambda)} \simeq 2U_\Sigma^{(\Lambda)} = 40\text{MeV}$. This yield $g_{\sigma^*\Lambda}/g_\sigma = g_{\sigma^*\Sigma}/g_\sigma = 0.69$, $g_{\sigma^*\Xi}/g_\sigma = 1.25$ [51].

Due to the scarcity of experimental data and theoretical calculations regarding the Δ resonance, there is uncertainty in the coupling parameters between the Δ resonances and meson fields(σ, ω, ρ). Therefore, we

limit ourselves to considering only the couplings with the σ meson field, which has been explored in the literature [52, 53]. We assume that the scalar coupling ratio $x_{\sigma\Delta} = g_{\sigma\Delta}/g_{\sigma N} > 1$ and choose a value close to the mass ratio of the Δ and the nucleon [54]. We adopt three different choices for $x_{\sigma\Delta}$ ($x_{\sigma\Delta} = 1.05$, $x_{\sigma\Delta} = 1.1$, and $x_{\sigma\Delta} = 1.15$) [55]. For $x_{\omega\Delta}$ and $x_{\rho\Delta}$, we take $x_{\omega\Delta} = g_{\omega\Delta}/g_{\omega N} = 1.1$ (Because we found that $x_{\omega\Delta} < 1$ would lead to a significantly lower maximum mass of neutron stars than astronomical observations.) and $x_{\rho\Delta} = g_{\rho\Delta}/g_{\rho N} = 1$ [56].

When neutrinos are not captured, the set of equilibrium chemical potential relations under general conditions is as follows::

$$\mu_i = \mu_n - q_i \mu_e \tag{6}$$

where q_i is the charge of i -th baryon, and the charge neutrality condition is fulfilled by:

$$\sum_B q_B \rho_B + \sum_D q_D \rho_D - \rho_e - \rho_\mu = 0 \tag{7}$$

The chemical potential of baryons, Δ and leptons read:

$$\mu_i = \sqrt{k_F^i{}^2 + m_i^{*2}} + g_{\omega i} \omega + g_{\phi i} \phi + g_{\rho i} \tau_{3i} \rho, i = B, D \tag{8}$$

$$\mu_l = \sqrt{k_F^l{}^2 + m_l^2}, \tag{9}$$

where k_F^i is the Fermi momentum and the m_i^* is the effective mass of baryon and Δ resonances, which can be related to the scalar meson field as $m_i^* = m_i - g_{\sigma i} \sigma - g_{\sigma^* i} \sigma^*$, and k_F^l is the Fermi momentum of the lepton $l(\mu^-, e^-)$.

TABLE II. Parameter sets for the IUFSU model discussed in the text and the meson masses $M_\sigma = 491.5\text{MeV}$, $M_\omega = 786\text{MeV}$, $M_\rho = 763\text{MeV}$.

Model	g_σ	g_ω	g_ρ	κ	λ	ξ	Λ_ν
IUFSU	9.9713	13.0321	13.5899	3.37685	0.000268	0.03	0.046

TABLE III. scalar meson hyperon coupling constants for IUFSU.

	Λ	Σ	Ξ
$x_{\sigma Y}$	0.615796	0.45219	0.305171

The total energy density can be given as

$$\begin{aligned}
\varepsilon_{B,D} = & \sum_{i=B,D} \frac{\gamma}{(2\pi)^3} \int_0^{k_{Fi}} \sqrt{m_i^* + k^2} d^3k + \frac{1}{2} m_\omega^2 \omega^2 \\
& + \frac{\xi}{8} g_{\omega N}^4 \omega^4 + \frac{1}{2} m_\sigma^2 \sigma^2 + \frac{\kappa}{6} g_{\sigma N}^3 \sigma^3 + \frac{\lambda}{24} g_{\sigma N}^4 \sigma^4 \\
& + \frac{1}{2} m_\rho^2 \rho^2 + 3\Lambda_\nu g_{\rho N}^2 g_{\omega N}^2 \omega^2 \rho^2 + \frac{1}{2} m_\phi^2 \phi^2 \\
& + \frac{1}{2} m_{\sigma^*}^2 \sigma^{2*} + \frac{1}{\pi^2} \sum_l \int_0^{k_{Fl}} \sqrt{k^2 + m_l^2} k^2 dk,
\end{aligned} \tag{10}$$

And the expression of pressure reads

$$P = \sum_{i=B,D} \mu_i \rho_i + \sum_{l=\mu,e} \mu_l \rho_l - \varepsilon, \tag{11}$$

Once the equation of state is specified, the mass-radius relation and other relevant quantities of neutron star can be obtained by solving the Tolman-Oppenheimer-Volkoff (TOV) equation [57].

$$\begin{aligned}
\frac{dP(r)}{dr} = & -\frac{GM(r)\varepsilon}{r^2} \left(1 + \frac{P}{\varepsilon C^2}\right) \left(1 + \frac{4\pi r^3 P}{M(r)C^2}\right) \\
& \times \left(1 - \frac{2GM(r)}{rC^2}\right)^{-1},
\end{aligned} \tag{12}$$

$$dM(r) = 4\pi r^2 \varepsilon(r) dr \tag{13}$$

The tidal deformability of a neutron star is reduced as a dimensionless form [58, 59].

$$\Lambda = \frac{2}{3} k_2 C^{-5} \tag{14}$$

where $C = GM/R$, the second Love number k_2 can be fixed simultaneously with the structures of compact stars [60].

The σ -cut scheme [33] involves introducing an additional sigma self-interaction term in the model [33, 61, 62], which results in a stiffer equation of state (EOS):

$$\Delta U(\sigma) = \alpha \ln(1 + \exp[\beta(f - f_{s,core})]) \tag{15}$$

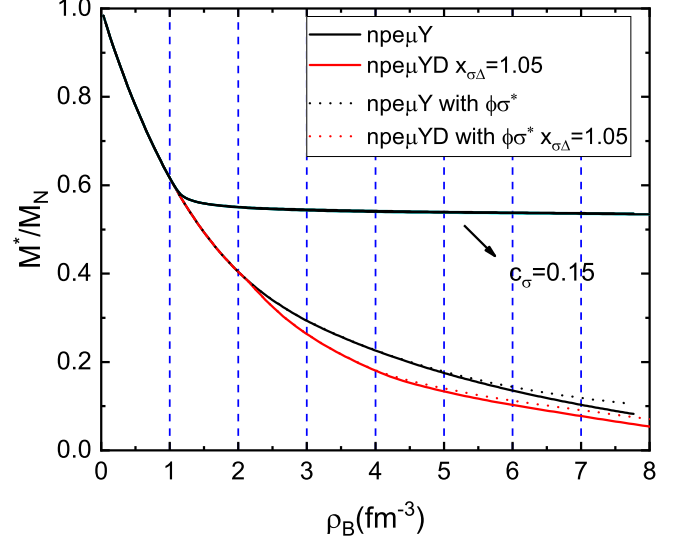


FIG. 1. Effective mass of nucleons versus baryon density in NS matter using and not using σ -cut scheme with considering σ^* and ϕ or not.

In this context, $f = g_{\sigma N} \sigma / M_N$ and $f_{s,core} = f_0 + c_\sigma(1 - f_0)$. Here, M_N represents the nucleon mass, and f_0 is the value of f at saturation density, which equals 0.31 in the IUFSU model. c_σ is a positive parameter that we can adjust. The smaller the value of c_σ , the stronger the effect of the σ -cut scheme. In our previous work, we extensively discussed the choice of the parameter c_σ [43]. In this paper, we adopt $c_\sigma = 0.15$ to satisfy the constraint on the maximum mass. The constants α and β have values of $4.822 \times 10^{-4} M_N^4$ and 120, respectively, following the settings in Ref. [33]. This scheme stiffens the equation of state by quenching the decrease of the effective nucleon mass $M_N^* = M_N(1 - f)$ above saturation density ρ_0 .

III. RESULTS

First, we studied the effect of the σ -cut scheme on the IUFSU model. In Fig. 1, we plot the ratio of the effective mass to the rest mass of nucleons as function of the baryon density. The dashed and solid lines represent the cases with and without strange mesons σ^* and ϕ , respectively. Here, ρ_0 is the saturation density, and we chose $x_{\sigma\Delta} = 1.05$ to consider the Δ resonance. We can observe that when $\rho \leq \rho_0$, the effective mass is almost the same as in nucleons-only matter and remains unchanged

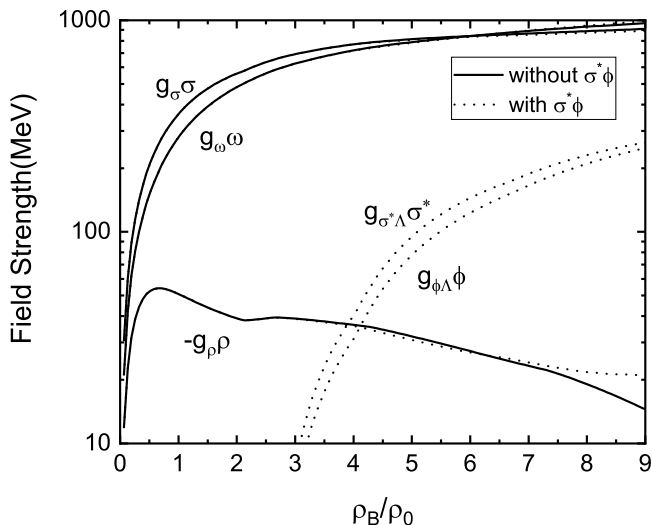


FIG. 2. Field strength of various mesons with considering σ^* and ϕ or not.

TABLE IV. Threshold densities n_{cr} (in units of ρ/ρ_0) for Δ resonance in dense nuclear matter for different values of $x_{\sigma\Delta}$ without σ -cut scheme.

Δ	n_{cr} (without $\sigma^*\phi$)/(with $\sigma^*\phi$)		
	$x_{\sigma\Delta} = 1.05$	$x_{\sigma\Delta} = 1.1$	$x_{\sigma\Delta} = 1.15$
Δ^{++}	/	7.54/7.73	6.27/6.24
Δ^+	8.60/8.83	6.53/6.60	5.01/5.04
Δ^0	6.53/6.66	4.49/4.56	3.52/3.55
Δ^-	2.13/2.13	1.90/1.90	1.74/1.74

by the σ -cut scheme. This suggests that the scheme does not alter the properties of nuclear matter at saturation, which is crucial. The inclusion of strange mesons σ^* and ϕ slightly slows down the drop in effective mass M^* , but this effect disappears when the σ -cut scheme is applied. However, when $\rho > \rho_0$, the effective mass drops to around $0.55M_N$, significantly suppressing the strength of the σ meson field strength. This is precisely the desired effect achieved by using the σ -cut scheme.

The field strength of various mesons are shown in Fig. 2. When the baryon density is approximately $3\rho_0$, the σ^* and ϕ mesons emerge, while the field strength of σ and ω mesons remains nearly unchanged. However, the field strength of the ρ meson increases in the high-density region ($6.6\rho_0$). And we also distinctly see from Fig. 2, the field strength of σ^* is larger than ϕ and both increase with the baryon density. When we choose σ -cut scheme (Fig. 3), the field strength of σ meson is truncated, and the field strength of the ρ meson decreases around $4\rho_0 \sim 6\rho_0$, and subsequently surpasses the case when strange mesons are included, additionally, the strength of strange mesons will also slightly increase. In RMF theory, the scalar meson σ and σ^* provides attraction, the vector meson ω and ϕ provides repulsion, these changes in meson strength may give the stiffer EOS.

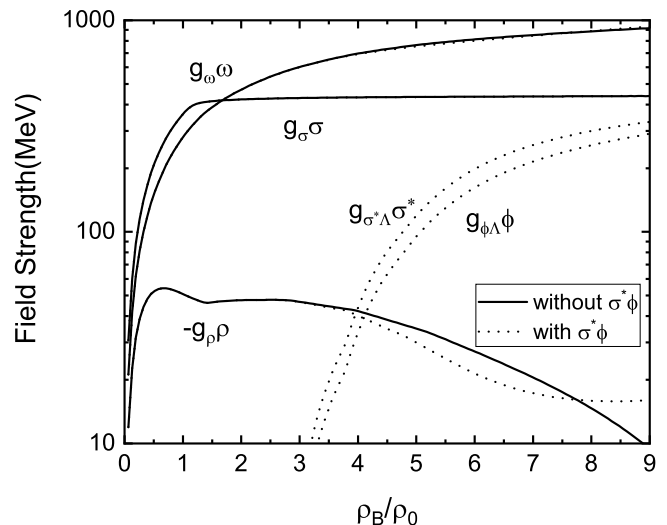


FIG. 3. Field strength of various mesons with considering σ^* and ϕ or not, $c_\sigma=0.15$

Fig. 4 illustrates the relative population of particles as a function of baryon density for different values of $x_{\sigma\Delta}$, namely $x_{\sigma\Delta} = 1.05, 1.1, 1.15$. The dashed and solid lines represent the cases with and without considering strange mesons (σ^* , ϕ), respectively. When the strange mesons are taken into account, the critical densities of Ξ^0 , Ξ^- , and Δ^{++} shift towards lower density regions, while the critical densities of Δ^+ and Δ^0 shift towards higher density regions. Additionally, with the increase of $x_{\sigma\Delta}$, the critical densities of Λ^0 , Ξ^0 , and Ξ^- move towards higher density regions, whereas the critical densities of leptons move towards lower density regions. Notably, as $x_{\sigma\Delta}$ increases, the Δ^{++} resonance starts to appear, and the overall critical density for the Δ resonance decreases, pushing the appearance of hyperons to lower density regions. Regarding the critical density of Δ resonance we have placed in Table IV.

Next we examine the effect of the σ -cut scheme on the particle population, this is plotted in the Fig. 5. As the decrease of μ^- , the Δ^+ and Δ^{++} increase as the charge balance conditions lead to the increase of Ξ^- and Δ^- , suggesting that baryons are more favorable as neutralizers of positive charges compared to leptons. As $x_{\sigma\Delta}$ increases from 1.05 to 1.15, the critical value of Δ resonance shifts to lower density while the critical density of hyperons move toward the high density region, in particular. When $x_{\sigma\Delta} = 1.15$, the critical density of Δ^0 moves before the Λ^0 . Although the σ -cut scheme significantly affects the critical density distribution of various particles, it does not change the relationship between the Δ resonance and strange mesons (σ^* , ϕ) as $x_{\sigma\Delta}$ varies.

Fig. 6 shows the pressure as a function of energy density in neutron star matter containing Δ resonances without the σ -cut scheme. The dashed line represents the case when strange mesons σ^* and ϕ are considered, while the solid line represents the case without consid-

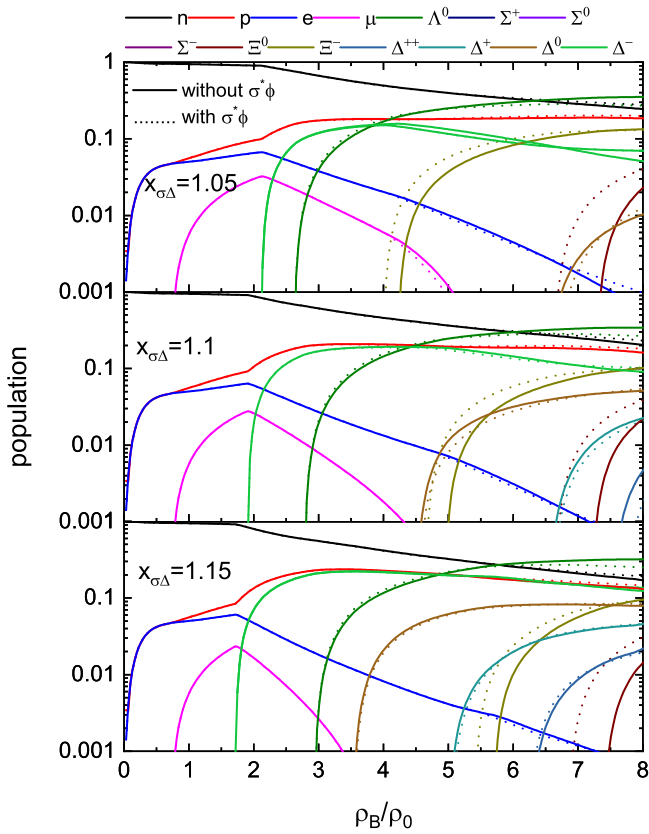


FIG. 4. Relative population of particles versus baryon density without σ -cut scheme with considering σ^* and ϕ or not, $x_{\sigma\Delta}=1.05$, $x_{\sigma\Delta}=1.1$, $x_{\sigma\Delta}=1.15$.

ering strange mesons. Although not particularly significant in the low-energy density region, in the high-energy density region, the presence of strange mesons slightly stiffens the equation of state due to their attractive effect. As $x_{\omega\Delta}$ increases, the equation of state becomes softer in the energy density range from $300\text{MeV}/f\text{m}^3$ to $600\text{MeV}/f\text{m}^3$. However, for energy density greater than $600\text{MeV}/f\text{m}^3$, it becomes significantly stiffer compared to the case when only hyperons are included. This suggests the existence of a softer equation of state in the low-density region, which ultimately constrains the radius of the neutron star, while the maximum mass does not show significant changes.

When considering the σ -cut scheme, we plot the equation of state (EOS) in Fig. 7, where the dashed and solid lines represent the cases with and without strange mesons, respectively. We can observe that the σ -cut scheme significantly stiffens the EOS, and this is due to the truncation of the σ meson field strength as shown in Fig. 3. Interestingly, in this case, the inclusion of strange mesons actually softens the EOS in the high-energy density region. Moreover, the σ -cut scheme retains the softening feature of the EOS in the low-density region. Compared to the case without the σ -cut scheme, the softening region shifts by approximately $50\text{MeV}/f\text{m}^3$ towards the

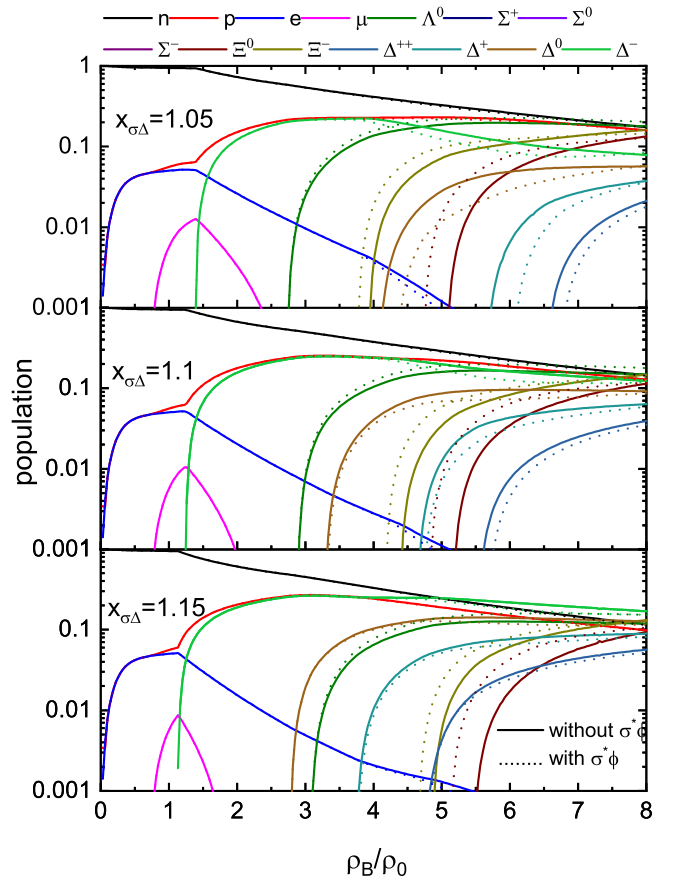


FIG. 5. Relative population of particles versus baryon density with considering σ^* and ϕ or not, and $c_\sigma = 0.15$, $x_{\sigma\Delta}=1.05$, $x_{\sigma\Delta}=1.1$, $x_{\sigma\Delta}=1.15$.

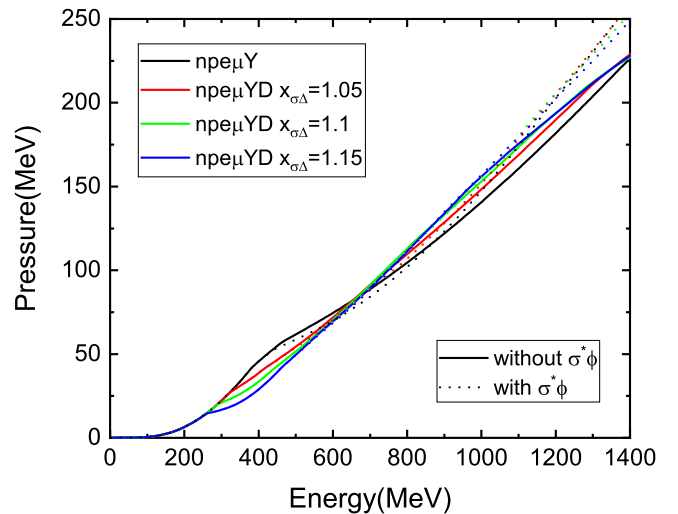


FIG. 6. Pressure versus energy density without the σ -cut scheme. The black solid line is for n, p, leptons and hyperons whereas others are with additional Δ resonance, dotted lines contain σ^* and ϕ mesons.

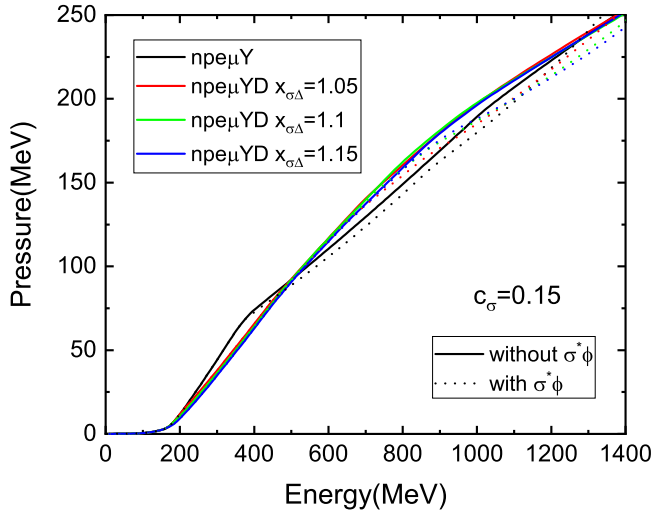


FIG. 7. Pressure versus energy density with the σ -cut scheme ($c_\sigma = 0.15$). The black solid line is for n, p, leptons and hyperons whereas others are with additional Δ resonance, dotted lines contain σ^* and ϕ mesons.

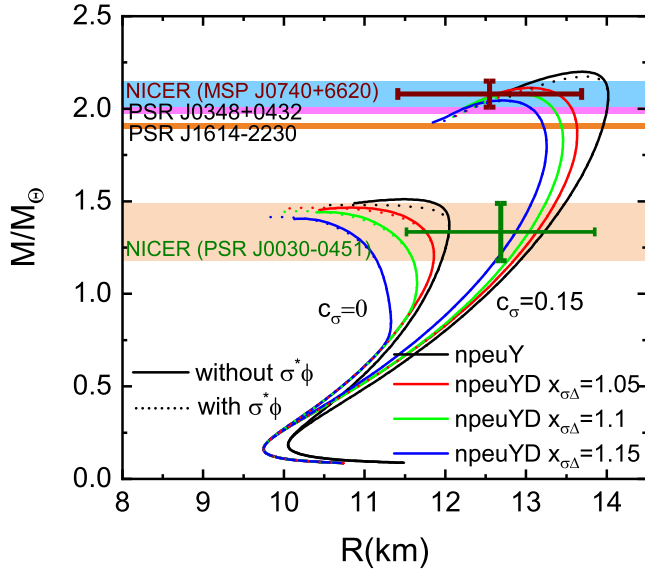


FIG. 8. Mass-radius relation using and not using σ -cut scheme in NS matter including hyperons and Δ resonance, the dotted line indicates that considering σ^* and ϕ . The horizontal bars indicate the observational constraints of PSR J1614 - 2230 [1–4], PSR J0348 + 0432 [5], MSP J0740 + 6620 [6] and PSR J0030-0451 [63].

low-density region. By obtaining the EOS through this approach, we can solve the TOV equation to produce neutron stars with masses up to $2M_\odot$, effectively eliminating the “hyperon puzzle.”

The mass-radius relationship for neutron stars (NS) discussed here and depicted in Fig. 8. The shaded bands represent the constraints imposed by the observables of massive neutron stars, namely PSR J1614-2230 [1–4] and

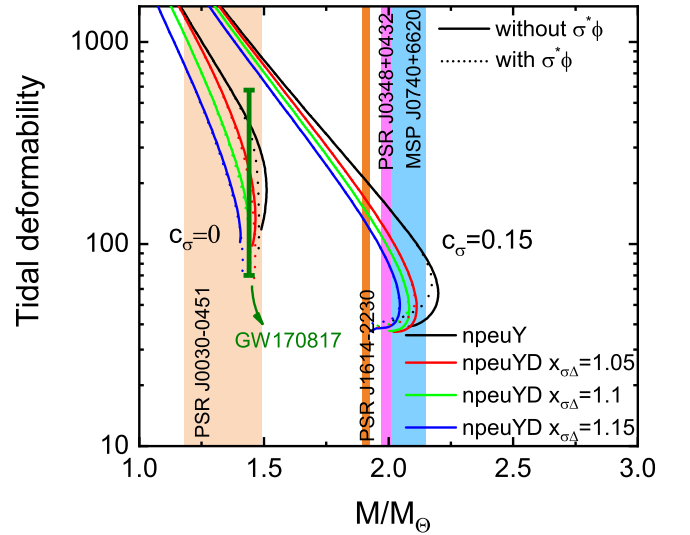


FIG. 9. The dimensionless tidal deformability as a function of star mass. The solid line indicates without σ -cut scheme, the dotted line indicates that considering σ^* and ϕ . And the constraints from GW170817 event for tidal deformability is shown.

PSR J034+0432 [5]. In 2019, the Neutron Star Interior Composition Explorer (NICER) collaboration reported precise measurements of the mass and radius of PSR J0030+0451 [63], and in 2021, they reported on MSP J0740+6620 [6]. The left solid lines in the figure, without σ -cut, demonstrate that different coupling parameters $x_{\sigma\Delta}$ have a notable impact on the maximum mass and radius of the neutron star. It reveals that the Δ resonance decreases the maximum mass and radius of the neutron star. As $x_{\sigma\Delta}$ increases (from 1.05 to 1.15), the maximum mass decreases. The right solid lines represent $c_\sigma = 0.15$, which significantly boosts the maximum mass of the neutron star beyond $2M_\odot$, in agreement with the constraints from gravitational waves and NICER (MSP J0740+6620). However, there is no significant difference between the maximum mass and radius variation of neutron stars with the addition of σ^* and ϕ . Table V presents the simultaneous measurements of the radius for MSP J0740+6620 and PSR J0030-0451 using NICER data, along with the maximum mass of the neutron star for various values of $x_{\sigma\Delta}$.

Another important constraint is the tidal deformability of the compact stars. In Fig. 9 we present the tidal deformabilities of compact stars corresponding to those in Fig. 8. Based on the gravitational wave data from the binary neutron star merger event GW170817, the tidal deformability at $1.4M_\odot$ was extracted as $\Lambda_{1.4} = 190^{+390}_{-120}$ [64]. From the figure, it is evident that the σ -cut scheme with a stiffer equation of state (EOS) yields larger values of $\Lambda_{1.4}$ and heavier masses. However, these values of $\Lambda_{1.4}$ fall outside the constraint set by GW170817. On the other hand, the softer EOS, without the σ -cut scheme, satisfies the GW170817 constraint, resulting in smaller

TABLE V. The maximum mass(in unit of solar mass M_\odot), central energy density ρ_c (in unit of ρ/ρ_0) and radius(km) in NS matter including hyperons and Δ resonance using and not using σ -cut scheme.

	without σ -cut			$c_\sigma=0.15$			MSP J0740+6620 [6]		PSR J0030-0451 [8]	
	M	ρ_c	R	M	ρ_c	R	M	R	M	R
(n, p, Y)	1.46	7.76	10.65	2.15	3.84	13.79				
$x_{\sigma\Delta} = 1.05(n, p, Y, D)$	1.45	7.76	10.62	2.08	4.4	13.3				
$x_{\sigma\Delta} = 1.1(n, p, Y, D)$	1.43	8.09	10.42	2.06	4.53	13.1	2.08 ± 0.07	$12.39^{+1.3}_{-0.98}$	$1.34^{+0.15}_{-0.16}$	$12.71^{+1.14}_{-1.19}$
$x_{\sigma\Delta} = 1.15(n, p, Y, D)$	1.40	8.6	10.1	2.02	4.66	12.91				

radii. Additionally, the inclusion of the Δ resonance maintains $\Lambda_{1.4}$ within the bounds of GW170817. These findings indicate that considering the Δ resonance in the softer EOS is necessary, given the strong constraint imposed by the observational tidal deformability of compact stars during the GW170817 event. Furthermore, future gravitational wave events from binary neutron star mergers are expected to provide measurements of the neutron star's tidal deformability at $2.0M_\odot$.

IV. SUMMARY

In this paper, we have discussed the Δ resonance and strange mesons (σ^* , ϕ) within neutron stars under the IUFSU model, prompted by recent astronomical observations yielding rapid results on the radii and tidal deformations of compact stars. However, the maximum masses of neutron stars generated by the softer equation of state (EOS) (known as the hyperon puzzle) fail to approach $2.0M_\odot$, thereby not satisfying the constraints from observations of massive neutron stars. Consequently, we employ the σ -cut scheme, resulting in a maximum mass exceeding $2M_\odot$.

We investigated the impact of strange mesons on neutron stars and found that within a neutron star, σ^* and ϕ mesons shift the critical density of hyperons towards the low-density region. However, with the inclusion of the Δ resonance, strange mesons lead to a shift of the critical density of the Δ resonance towards the high-density region. As the coupling parameter $x_{\sigma\Delta}$ increases, the Δ resonance appears earlier, suggesting that the presence of strange mesons affects the critical density of the Δ resonance. These results indicate that although σ^*

and ϕ only interact with hyperons, considering the Δ resonance, they play a minor role in the interaction confinement between baryons. Additionally, the inclusion of strange mesons slightly increases the mass, but the variations are not significant. Interestingly, when the σ -cut scheme is considered, σ^* and ϕ mesons lead to a softening of the equation of state.

Furthermore, we explore the effect of $x_{\sigma\Delta}$ on the Δ resonance. For the Δ coupling constants, we consider $x_{\sigma\Delta} = 1.05, 1.1, \text{ and } 1.15$. The value of $x_{\sigma\Delta}$ significantly influences the relative population of particles as a function of the baryon density. We observe that the inclusion of the Δ resonance shifts the critical density of hyperons towards the high-density region as $x_{\sigma\Delta}$ increases from 1.05 to 1.15, while the critical density of the Δ resonance moves towards the low-density region, this suggests that an early appearance of the Δ resonance may contribute to the stability of neutron stars. Furthermore, with increasing $x_{\sigma\Delta}$, the equation of state softens in the low-density region, resulting in a significant reduction in the radius of neutron stars, while the maximum mass remains almost unchanged.

When not using the σ -cut scheme, the softer equation of state considering the Δ resonance still falls within the $\Lambda_{1.4}$ range of GW170817 and results in smaller radii. And when we employ the σ -cut scheme with $c_\sigma = 0.15$, we observe that the maximum mass and radius of neutron stars obtained align closely with the constraints from NICER (MSP J0740+6620). However, the tidal deformability exceeds the constraint from GW170817, for neutron stars with a mass exceeding $2M_\odot$, future gravitational wave events from binary neutron star mergers may provide new constraints on tidal deformability.

-
- | | |
|----------------------------------------------------------------------------------------------------------------------------------------------------------------------------------------------------------------------------------------------------------------------------------------------------------------------------------------------------------------------------------------------------------------------------------------------------------------------------------------------------------------------------------------|-----------------------------------------------------------------------------------------------------------------------------------------------------------------------------------------------------------------------------------------------------------------------------------------------------------------------------------------------------------------------------------------------------------------------------------------------------------------------------------------------------------------------------------------------|
| <p>[1] Paul Demorest, Tim Pennucci, Scott Ransom, Mallory Roberts, and Jason Hessels. Shapiro Delay Measurement of A Two Solar Mass Neutron Star. <i>Nature</i>, 467:1081–1083, 2010.</p> <p>[2] Zaven Arzoumanian et al. The NANOGrav 11-year Data Set: High-precision timing of 45 Millisecond Pulsars. <i>Astrophys. J. Suppl.</i>, 235(2):37, 2018.</p> <p>[3] Emmanuel Fonseca et al. The NANOGrav Nine-year Data Set: Mass and Geometric Measurements of Binary Millisecond Pulsars. <i>Astrophys. J.</i>, 832(2):167, 2016.</p> | <p>[4] Feryal Ozel, Dimitrios Psaltis, Scott Ransom, Paul Demorest, and Mark Alford. The Massive Pulsar PSR J1614-2230: Linking Quantum Chromodynamics, Gamma-ray Bursts, and Gravitational Wave Astronomy. <i>Astrophys. J. Lett.</i>, 724:L199–L202, 2010.</p> <p>[5] John Antoniadis, Paulo CC Freire, Norbert Wex, Thomas M Tauris, Ryan S Lynch, Marten H Van Kerkwijk, Michael Kramer, Cees Bassa, Vik S Dhillon, Thomas Driebe, et al. A massive pulsar in a compact relativistic binary. <i>Science</i>, 340(6131):1233232, 2013.</p> |
|----------------------------------------------------------------------------------------------------------------------------------------------------------------------------------------------------------------------------------------------------------------------------------------------------------------------------------------------------------------------------------------------------------------------------------------------------------------------------------------------------------------------------------------|-----------------------------------------------------------------------------------------------------------------------------------------------------------------------------------------------------------------------------------------------------------------------------------------------------------------------------------------------------------------------------------------------------------------------------------------------------------------------------------------------------------------------------------------------|

- [6] Emmanuel Fonseca, H Thankful Cromartie, Timothy T Pennucci, Paul S Ray, A Yu Kirichenko, Scott M Ransom, Paul B Demorest, Ingrid H Stairs, Zaven Arzumanyan, Lucas Guillemot, et al. Refined mass and geometric measurements of the high-mass psr j0740+ 6620. *The Astrophysical Journal Letters*, 915(1):L12, 2021.
- [7] H. T. Cromartie et al. Relativistic Shapiro delay measurements of an extremely massive millisecond pulsar. *Nature Astron.*, 4(1):72–76, 2019.
- [8] Thomas E Riley, Anna L Watts, Paul S Ray, Slavko Bogdanov, Sebastien Guillot, Sharon M Morsink, Anna V Bilous, Zaven Arzumanyan, Devarshi Choudhury, Julia S Deneva, et al. A nicer view of the massive pulsar psr j0740+ 6620 informed by radio timing and xmm-newton spectroscopy. *The Astrophysical Journal Letters*, 918(2):L27, 2021.
- [9] B. P. Abbott et al. Properties of the binary neutron star merger GW170817. *Phys. Rev. X*, 9(1):011001, 2019.
- [10] Michael W. Coughlin et al. Constraints on the neutron star equation of state from AT2017gfo using radiative transfer simulations. *Mon. Not. Roy. Astron. Soc.*, 480(3):3871–3878, 2018.
- [11] Jurgen Schaffner and Igor N. Mishustin. Hyperon rich matter in neutron stars. *Phys. Rev. C*, 53:1416–1429, 1996.
- [12] Chen Wu and Zhongzhou Ren. Strange hadronic stars in relativistic mean-field theory with the FSUGold parameter set. *Phys. Rev. C*, 83:025805, 2011.
- [13] G. F. Burgio, H. J. Schulze, I. Vidana, and J. B. Wei. Neutron stars and the nuclear equation of state. *Prog. Part. Nucl. Phys.*, 120:103879, 2021.
- [14] Domenico Logoteta. Hyperons in Neutron Stars. *Universe*, 7(11):408, 2021.
- [15] Ting-Ting Sun, Shi-Sheng Zhang, Qiu-Lan Zhang, and Cheng-Jun Xia. Strangeness and Δ resonance in compact stars with relativistic-mean-field models. *Phys. Rev. D*, 99(2):023004, 2019.
- [16] K. A. Maslov, E. E. Kolomeitsev, and D. N. Voskresensky. Δ resonances and charged ρ mesons in neutron stars. *J. Phys. Conf. Ser.*, 932(1):012040, 2017.
- [17] E. E. Kolomeitsev, K. A. Maslov, and D. N. Voskresensky. Delta isobars in relativistic mean-field models with σ -scaled hadron masses and couplings. *Nucl. Phys. A*, 961:106–141, 2017.
- [18] Armen Sedrakian and Arus Harutyunyan. Delta-resonances and hyperons in proto-neutron stars and merger remnants. *Eur. Phys. J. A*, 58(7):137, 2022.
- [19] Alessandro Drago, Andrea Lavagno, Giuseppe Pagliara, and Daniele Pigato. Early appearance of Δ isobars in neutron stars. *Phys. Rev. C*, 90(6):065809, 2014.
- [20] N. K. Glendenning. Neutron Stars Are Giant Hypernuclei? *Astrophys. J.*, 293:470–493, 1985.
- [21] Veronica Dexheimer, Kauan D. Marquez, and Débora P. Menezes. Delta baryons in neutron-star matter under strong magnetic fields. *Eur. Phys. J. A*, 57(7):216, 2021.
- [22] K. D. Marquez, M. R. Pelicer, S. Ghosh, J. Peterson, D. Chatterjee, V. Dexheimer, and D. P. Menezes. Exploring the effects of Δ baryons in magnetars. *Phys. Rev. C*, 106(3):035801, 2022.
- [23] Torsten Schürhoff, Stefan Schramm, and Veronica Dexheimer. Neutron stars with small radii—the role of Δ resonances. *The Astrophysical Journal Letters*, 724(1):L74, nov 2010.
- [24] Vivek Baruah Thapa and Monika Sinha. Dense matter equation of state of a massive neutron star with antikaon condensation. *Phys. Rev. D*, 102(12):123007, 2020.
- [25] Toshiaki Maruyama, Toshitaka Tatsumi, Dmitri N. Voskresensky, Tomonori Tanigawa, Tomoki Endo, and Satoshi Chiba. Finite size effects on kaonic pasta structures. *Phys. Rev. C*, 73:035802, 2006.
- [26] G. E. Brown, Chang-Hwan Lee, Hong-Jo Park, and Manque Rho. Study of strangeness condensation by expanding about the fixed point of the Harada-Yamawaki vector manifestation. *Phys. Rev. Lett.*, 96:062303, 2006.
- [27] Guo-yun Shao and Yu-xin Liu. Influence of the isovector-scalar channel interaction on neutron star matter with hyperons and antikaon condensation. *Phys. Rev. C*, 82:055801, 2010.
- [28] Prasanta Char and Sarmistha Banik. Massive Neutron Stars with Antikaon Condensates in a Density Dependent Hadron Field Theory. *Phys. Rev. C*, 90(1):015801, 2014.
- [29] GF Burgio, H-J Schulze, A Li, et al. Hyperon stars at finite temperature in the brueckner theory. *Physical Review C*, 83(2):025804, 2011.
- [30] Diego Lonardonì, Alessandro Lovato, Stefano Gandolfi, and Francesco Pederiva. Hyperon Puzzle: Hints from Quantum Monte Carlo Calculations. *Phys. Rev. Lett.*, 114(9):092301, 2015.
- [31] Ignazio Bombaci. The Hyperon Puzzle in Neutron Stars. *JPS Conf. Proc.*, 17:101002, 2017.
- [32] N. K. Glendenning and S. A. Moszkowski. Reconciliation of neutron star masses and binding of the lambda in hypernuclei. *Phys. Rev. Lett.*, 67:2414–2417, 1991.
- [33] K. A. Maslov, E. E. Kolomeitsev, and D. N. Voskresensky. Making a soft relativistic mean-field equation of state stiffer at high density. *Phys. Rev. C*, 92(5):052801, 2015.
- [34] Luca Bonanno and Armen Sedrakian. Composition and stability of hybrid stars with hyperons and quark color-superconductivity. *Astronomy & Astrophysics*, 539:A16, 2012.
- [35] Giuseppe Colucci and Armen Sedrakian. Equation of state of hypernuclear matter: impact of hyperon–scalar-meson couplings. *Phys. Rev. C*, 87:055806, 2013.
- [36] M. Fortin, C. Providencia, A. R. Raduta, F. Gulminelli, J. L. Zdunik, P. Haensel, and M. Bejger. Neutron star radii and crusts: uncertainties and unified equations of state. *Phys. Rev. C*, 94(3):035804, 2016.
- [37] Yanjun Chen, Hua Guo, and Yuxin Liu. Neutrino scattering rates in neutron star matter with Delta isobars. *Phys. Rev. C*, 75:035806, 2007.
- [38] Jia Jie Li, Armen Sedrakian, and Mark Alford. Relativistic hybrid stars with sequential first-order phase transitions and heavy-baryon envelopes. *Phys. Rev. D*, 101(6):063022, 2020.
- [39] Jia Jie Li and Armen Sedrakian. Implications from gw170817 for δ -isobar admixed hypernuclear compact stars. *The Astrophysical Journal Letters*, 874(2):L22, 2019.
- [40] Isaac Vidaña. Hyperons and neutron stars. *Nucl. Phys. A*, 914:367–376, 2013.
- [41] T. Klähn, R. Lastowiecki, and D. B. Blaschke. Implications of the measurement of pulsars with two solar masses for quark matter in compact stars and heavy-ion collisions: A Nambu–Jona-Lasinio model case study. *Phys. Rev. D*, 88(8):085001, 2013.
- [42] M. Bhuyan, Shan-Gui Zhou, S. K. Patra, and B. V. Carlson. The attribute of rotational profile to the hyperon puzzle in the prediction of heaviest compact star. *Int. J.*

- Mod. Phys. E*, 26(09):1750052, 2017.
- [43] Fu Ma, Wenjun Guo, and Chen Wu. Kaon meson condensate in neutron star matter including hyperons. *Phys. Rev. C*, 105(1):015807, 2022.
- [44] Fei Wu and Chen Wu. Hyperonized neutron stars within the framework of the σ -cut scheme. *Eur. Phys. J. A*, 56(1):20, 2020.
- [45] F. J. Fattoyev, C. J. Horowitz, J. Piekarewicz, and G. Shen. Relativistic effective interaction for nuclei, giant resonances, and neutron stars. *Phys. Rev. C*, 82:055803, 2010.
- [46] Fabrizio Grill, Helena Pais, Constança Providência, Isaac Vidaña, and Sidney S. Avancini. Equation of state and thickness of the inner crust of neutron stars. *Phys. Rev. C*, 90(4):045803, 2014.
- [47] Jurgen Schaffner, Carl B. Dover, Avraham Gal, Carsten Greiner, D. John Millener, and Horst Stoecker. Multiply strange nuclear systems. *Annals Phys.*, 235:35–76, 1994.
- [48] Jinniu Hu, Ying Zhang, and Hong Shen. The Ξ -nuclear potential constrained by recent Ξ^- hypernuclei experiments. *J. Phys. G*, 49(2):025104, 2022.
- [49] M. Fortin, S. S. Avancini, C. Providência, and I. Vidaña. Hypernuclei and massive neutron stars. *Phys. Rev. C*, 95(6):065803, 2017.
- [50] P. Khaustov et al. Evidence of Xi hypernuclear production in the C-12(K-,K+)(Xi)Be-12 reaction. *Phys. Rev. C*, 61:054603, 2000.
- [51] Jurgen Schaffner, Carl B. Dover, Avraham Gal, Carsten Greiner, and Horst Stoecker. Strange hadronic matter. *Phys. Rev. Lett.*, 71:1328–1331, 1993.
- [52] Zhu-Xia Li, Guang-Jun Mao, Yi-Zhong Zhuo, and W. Greiner. Transition to Delta matter from hot, dense nuclear matter within a relativistic mean field formulation of the nonlinear sigma and omega model. *Phys. Rev. C*, 56:1570–1575, 1997.
- [53] Xue-min Jin. QCD sum rules for delta isobar in nuclear matter. *Phys. Rev. C*, 51:2260–2263, 1995.
- [54] D. S. Kosov, C. Fuchs, B. V. Martemyanov, and A. Faessler. Constraints on the coupling constants of Sigma and Omega mesons to Delta isobars. *Phys. Lett. B*, 421:37–40, 1998.
- [55] Alessandro Drago, Andrea Lavagno, and Giuseppe Pagliara. Can very compact and very massive neutron stars both exist? *Phys. Rev. D*, 89(4):043014, 2014.
- [56] Vivek Baruah Thapa, Monika Sinha, Jia Jie Li, and Armen Sedrakian. Massive Δ -resonance admixed hypernuclear stars with antikaon condensations. *Phys. Rev. D*, 103(6):063004, 2021.
- [57] M. Baldo, I. Bombaci, and G. F. Burgio. Microscopic nuclear equation of state with three-body forces and neutron star structure. *Astron. Astrophys.*, 328:274–282, 1997.
- [58] Tanja Hinderer. Tidal love numbers of neutron stars. *The Astrophysical Journal*, 677(2):1216, 2008.
- [59] Sergey Postnikov, Madappa Prakash, and James M. Lattimer. Tidal Love Numbers of Neutron and Self-Bound Quark Stars. *Phys. Rev. D*, 82:024016, 2010.
- [60] Tanja Hinderer, Benjamin D. Lackey, Ryan N. Lang, and Jocelyn S. Read. Tidal deformability of neutron stars with realistic equations of state and their gravitational wave signatures in binary inspiral. *Phys. Rev. D*, 81:123016, 2010.
- [61] Young-Ho Song, Rimantas Lazauskas, and Vladimir Gudkov. Time Reversal Invariance Violating and Parity Conserving effects in Neutron Deuteron Scattering. *Phys. Rev. C*, 84:025501, 2011. [Erratum: Phys.Rev.C 93, 049901 (2016)].
- [62] E. E. Kolomeitsev, K. A. Maslov, and D. N. Voskresensky. Hyperon puzzle and the RMF model with scaled hadron masses and coupling constants. *J. Phys. Conf. Ser.*, 668(1):012064, 2016.
- [63] Thomas E Riley, Anna L Watts, Slavko Bogdanov, Paul S Ray, Renee M Ludlam, Sebastien Guillot, Zaven Arzumanian, Charles L Baker, Anna V Bilous, Deepto Chakrabarty, et al. A nicer view of psr j0030+ 0451: Millisecond pulsar parameter estimation. *The Astrophysical Journal Letters*, 887(1):L21, 2019.
- [64] B. P. Abbott et al. GW170817: Measurements of neutron star radii and equation of state. *Phys. Rev. Lett.*, 121(16):161101, 2018.